Science of the Total Environment 419 (2012) 170–177

Contents lists available at SciVerse ScienceDirect

Science of the Total Environment

journal homepage: www.elsevier.com/locate/scitotenv

Dispersion and stability of bare hematite nanoparticles: Effect of dispersion tools, nanoparticle concentration, humic acid and ionic strength

Dionne Dickson [a], Guangliang Liu [a], Chenzhong Li [b], Georgio Tachiev [c], Yong Cai [a,d,*]

[a] Department of Chemistry and Biochemistry, Florida International University, Miami, FL, 33199, USA
[b] Department of Biomedical Engineering, Florida International University, Miami, FL, 33174, USA
[c] Applied Research Center, Florida International University, Miami, FL, 33174, USA
[d] Southeast Environmental Research Center, Florida International University, Miami, FL, 33199, USA

ARTICLE INFO

Article history:
Received 26 October 2011
Received in revised form 22 December 2011
Accepted 8 January 2012
Available online 30 January 2012

Keywords:
Iron oxide nanoparticles (IONPs)
Probe ultrasonication
Dispersion
IONPs' stability
Ionic strength
Humic acid

ABSTRACT

The aggregation and sedimentation of iron oxide nanoparticles (IONPs) can significantly affect the mobility and reactivity of IONPs and subsequently influence the interaction between IONPs and environmental contaminants. Dispersing bare IONPs into a stable suspension within nanoscale range is an important step for studying the interaction of IONPs with contaminants (e.g., toxic metals). In this study, different techniques to disperse bare IONPs (vortex, bath sonication and probe ultrasonication) and the effects of important environmental factors such as dissolved organic matter and ionic strength on the stability of IONPs dispersions were investigated. Vortex minimally dispersed IONPs with hydrodynamic diameter outside the "nano-size range" (698–2400 nm). Similar to vortex, bath sonication could not disperse IONPs efficiently. Probe ultrasonication was more effective at dispersing IONPs (50% or more) with hydrodynamic diameters ranging from 120 to 140 nm with minimal changes in size and sedimentation of IONPs for a prolonged period of time. Over the course of 168 h, considerable amounts of IONPs remained dispersed in the presence and absence of low ionic strength (0.1 mM of NaCl) and 100 mg/L of humic acid (HA). These results indicate that IONPs can be broken down efficiently into "nanosize range" by probe ultrasonication and a degree of stability can be achieved without the use of synthetic modifiers to enhance colloidal stability. This dispersion tool could be used to develop a laboratory method to study the adsorption mechanism between dispersed bare IONPs and toxic contaminants.

1. Introduction

Groundwater pollution by heavy metals and organic pollutants has become an important issue globally and the development of inexpensive remediation technologies to clean up water is crucial. Nanotechnology has emerged as one of the leading technologies for cleaning up polluted sites. Currently, nanotechnology is widely studied and has shown considerable growth in the remediation of contaminants in ground and surface waters. Nanoscale zerovalent iron (NZVI) is considered as the first generation nanoscale environmental technologies and has the potential to remove a wide range of pollutants (Sun et al., 2006). NZVI has shown significant applications in groundwater remediation of chlorinated organic compounds such as trichloroethylene, organochlorine pesticides, polychlorinated biphenyls as well as remediation of toxic metals (Phenrat et al., 2007). In the past few years, a variety of iron oxide nanoparticles (IONPs) has been studied for environmental remediation purposes. These IONPs behave similarly to NZVI when used as treatment for contaminated sites and are frequently used as a model system for understanding aggregation behavior (He et al., 2008).

The growing interest in engineered NZVI and IONPs for groundwater remediation is attributed to the large surface area (25–54 m^2/g), highly reactive surface sites and high in-situ reactivity (Phenrat et al., 2007; Theron et al., 2008). The possibility of in-situ remediation results in shorter remediation time and low cost, as nanoscale metal particles are applied directly to contaminated sites (Wang and Zhang, 1997; He and Zhao, 2007). Despite the advantages, NZVI and IONPs have one major limitation that can be detrimental to their use as effective groundwater treatment. Studies have shown rapid agglomeration of NZVI and IONPs to form large aggregates that will sediment (He and Zhao, 2007). In the aquatic environment, aggregation of nanoparticles results from the interaction between nanoparticles surface and water components and is strongly influenced by several factors such as salinity, solution composition, surface chemistry, concentration of suspended particles, and the pH especially where the nanoparticles is approaching the pH of point zero charge (PZC)

---

* Corresponding author at: Department of Chemistry and Biochemistry, Florida International University, Miami, Florida, 33199, USA. Tel.: +1 305 348–6210; fax: +1 305 348 3772.
E-mail address: cai@fiu.edu (Y. Cai).

0048-9697/$ – see front matter © 2012 Elsevier B.V. All rights reserved.
doi:10.1016/j.scitotenv.2012.01.012

(Mylon et al., 2004; Yang et al., 2007; Baalousha, 2009; Hu et al., 2010). Particle–particle interactions are the major driving forces for aggregation and deposition of nanoparticles, though other interactions such as steric, magnetic and hydration forces can also contribute to the fore-told processes (Petosa et al., 2010). The Derjaguin–Landau–Verwey–Overbeek (DLVO) theory describes colloidal stability and can be used to explain the stability of nanoparticles in aquatic environment. The DLVO theory states that the stability of nanoparticles can be explained by the sum (total interaction energy) of van der Waals and electric double layer interactions (Deryagin and Landau, 1941; Verwey, 1947; Verwey and Overbeek, 1948; Petosa et al., 2010). The total interaction energy is experienced by a nanoparticle when it is approaching another particle and this energy determines whether the net interaction between particles are repulsive or attractive (Zhang et al., 2008). In addition, the Hamaker theory (Petosa et al., 2010) is an important component in the DLVO theory as the Hamaker constant relates the interatomic van der Waals interaction to the total van der Waals interaction.

Aggregation and sedimentation can significantly alter the mobility of the nanoparticles in aquatic environment and reduce the efficacy of using these nanoparticles for remediation purposes (Sun et al., 2007; Kim et al., 2009). Therefore, stable dispersions of nanoparticles are critical for efficient sorption of pollutants. In recent years, there is a noticeable increase in the application of modifiers, e.g., soluble polymers and surfactants, to alter the surface of nanoparticles thus preventing aggregation (Schrick et al., 2004; Kanel et al., 2007; Yang et al., 2007). Several researchers have reported the use of modifiers that are capable of reducing NZVI and IONPs aggregation (Schrick et al., 2004; He and Zhao, 2007; Kanel et al., 2007; Yang et al., 2007; Tiraferri et al., 2008). Although modifiers can enhance colloidal stability, they can be expensive, have adverse effect on the environment and alter the surface of the nanoparticles, thereby affecting the fate and transport of nanoparticles and their interaction with contaminants (Tiraferri et al., 2008). Specifically, modifiers could affect the sorption and desorption of contaminants, introduce additional mass transfer limitations of contaminants to active surface sites, and could decrease the reaction rate of the reactions that could be taking place at the surface (Phenrat et al., 2009). Phenrat et al. (2009) reported a decrease in dechlorination rate of trichloroethylene nonlinearly with increase surface modifiers on Fe^0/Fe_3O_4 nanoparticles. Natural surface modification can also occur by the adsorption of dissolved organic matter (DOM) on IONPs. DOM is ubiquitous in the environment and not only has the capability to adsorb onto IONPs but able to complex with heavy metals (Rangsivek and Jekel, 2008). The surface coating of IONPs with DOM can result in the nanoparticles becoming negatively charge thus preventing their aggregation in aqueous environment (Liu et al., 2008). With the increase in the use of engineered nanoparticles in remediation of environmental pollutants, it is critical to understand how these nanoparticles behave and interact with pollutants once they are introduced into the environment. As the first step, we need to develop a technique for preparing a stable dispersion of IONPs in a laboratory setting.

The goal of this research was to develop a method to disperse bare IONPs and to determine IONPs' stability after being dispersed and exposed to environmentally relevant conditions (pH 6–8 and in the presence of natural organic matter and ionic strength). The scope of this work was not to disperse large quantity of IONPs for real field practice. However, we intend to disperse IONPs in a laboratory setting to provide a tool to prepare a uniformly dispersed suspension. The purpose of preparing such a bare IONPs suspension was to estimate how nanomaterials might exist in the environment. This in turn will provide an in-depth understanding of how nanomaterials will behave in the environment with respect to the fate and transformation of contaminants. This study investigated and compared different mechanical methods to disperse hematite nanoparticles without the use of modifiers.

2. Materials and methods

2.1. Materials and chemicals

Commercial iron oxide nanoparticles (α-Fe_2O_3, 98% purity and 50 m^2/g specific surface area, primary particle diameter from 20 to 50 nm) were purchased from Nanostructured and Amorphous Materials (Houston, Texas). Humic acid (HA) was obtained from Acros Organic (New Jersey, USA) and sodium chloride was purchased from Fisher Scientific (New Jersey, USA). All materials were suspended or dissolved in nanopure 18.2 MΩ water produced from a nanopure diamond lab water system (Barnstead Thermolyne Corporation, Dubuque, IA) and prepared in Corning 50 mL polypropylene centrifuge tubes.

2.2. Instrumentation

Iron oxide nanoparticles were dispersed using a Fisher Scientific touch mixer model 232 (Pittsburgh, PA), Branson ultrasonic model 1510 (Danbury, CT) and Fisher Scientific sonic dismembrator model 100 (Pittsburg, PA). For particle size monitoring using dynamic light scattering (DLS), a Malvern Zetasizer Nano-ZS (Westborough, MA) was employed. The hydrodynamic diameters reported in this study represent the average particle diameter "z-average" intensity peak as a function of size. Zeta potential measurements were also made using the Malvern Zetasizer Nano-ZS. Total iron concentration was monitored using a graphite furnace atomic absorption spectrometer (GFAAS) (Perkin Elmer, model AAnalyst 600). The pH measurements were made using a Fisher Scientific accumet Research AR15 pH/mV/°C meter.

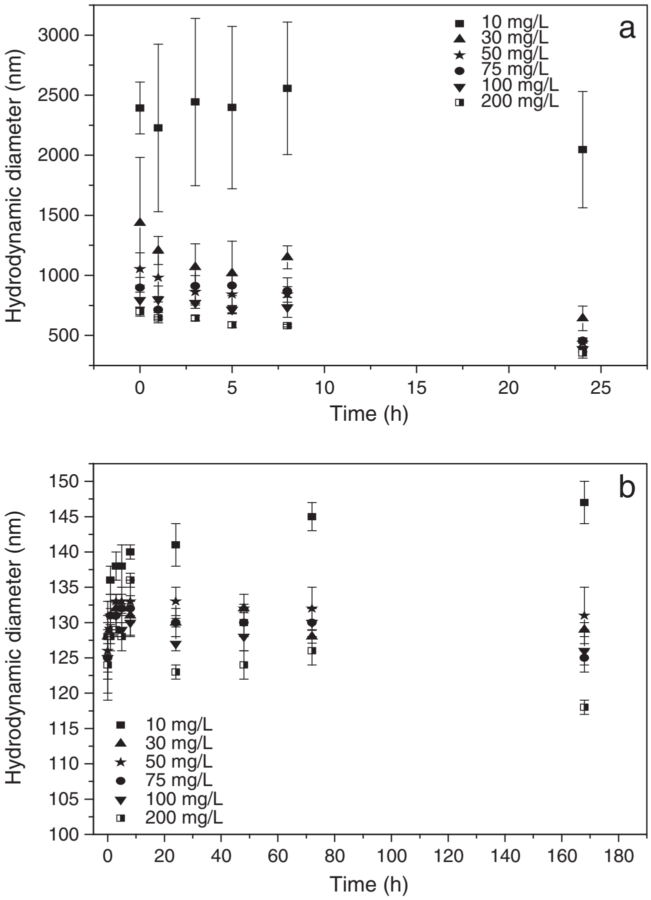

Fig. 1. The time dependent hydrodynamic diameter of 10, 30, 50, 75, 100 and 200 mg/L IONPs dispersed by a) vortex for 20 min at power level 10 and b) ultrasonic probe for 20 min at power level 6.

2.3. Experimental procedures

2.3.1. Effect of dispersion techniques on IONPs' stability

2.3.1.1. Dispersion of iron oxide nanoparticles. Stock suspension (40 mL) of α-Fe_2O_3 nanoparticles was prepared by mixing the required amount of α-Fe_2O_3 nanoparticles and nanopure water to make a concentration of 500 mg/L of α-Fe_2O_3 (IONPs). The stock suspension was dispersed using a vortex, bath sonication or probe ultrasonication to investigate which technique can provide sufficient power to disperse the nanoparticles. For vortexing, the stock suspension was vortexed for 20 min at the highest speed (speed 10). For bath sonication (power density of 0.0370 W/mL), the stock suspension was sonicated for 30 min. For ultrasonication, the following probe power and sonication times were investigated: probe power level 3 (power density of 0.275 W/mL) and level 6 (power density of 0.55 W/mL) at 5, 20 and 60 min of sonication for each power level. Immediately following sonication 20 mL of IONP suspensions (each containing 10, 30, 50, 75, 100 and 200 mg/L of α-Fe_2O_3) was prepared by subsequent dilution of the stock suspension. Time dependent hydrodynamic diameters of the nanoparticles were measured in triplicate at 0, 1, 3, 5, 8, 24, 48, 72 and 168 h with all sizes reported as mean ± standard deviation. Suspensions had pH ranging from 6.2 to 7.60. The drift in pH was a result of the suspensions not being buffered.

2.3.1.2. Iron analysis. Total iron concentration in the 10, 30, 50, 75, 100 and 200 mg/L IONPs suspensions was analyzed using GFAAS to monitor the sedimentation of IONPs over time. Before iron analysis, IONP suspension underwent acid digestion in 50% nitric acid for 20 min at 95 ± 5 °C.

2.3.2. Effect of humic acid (HA) and ionic strength on IONPs' stability

A 500 mg/L stock suspension (40 mL) of α-Fe_2O_3 nanoparticles was prepared and dispersed using probe ultrasonication for 20 min at power level 6. After probe sonication, concentrations of IONPs (10, 30, 50, 75, 100 and 200 mg/L) were prepared by subsequent dilution of the stock suspension and spiked with appropriate amount of HA to make a concentration of 100 mg/L HA. For the effect of ionic strength, the diluted IONP suspensions were spiked with the appropriate amount of NaCl to make a concentration of 0.1, 10 and 100 mM NaCl. In addition, the stability of IONPs was also investigated in the presence of both HA (100 mg/L) and NaCl (0.1 mM). For these experiments, DLS measurements and iron quantification were performed at 0, 1, 3, 5, 8, 24, 48, 72 and 168 h. Zeta potential measurements were performed while investigating the effect of HA alone on the aggregation behavior of IONPs. Zeta potential measurements could indicate whether HA is able to adsorb to IONPs resulting in a change in charge on the IONPs surface.

3. Results and discussion

3.1. Effect of dispersion techniques on IONPs' size distribution

Commercial grade nanoparticles are obtained as agglomerates and the breakage of IONPs to its primary particle size is an important step

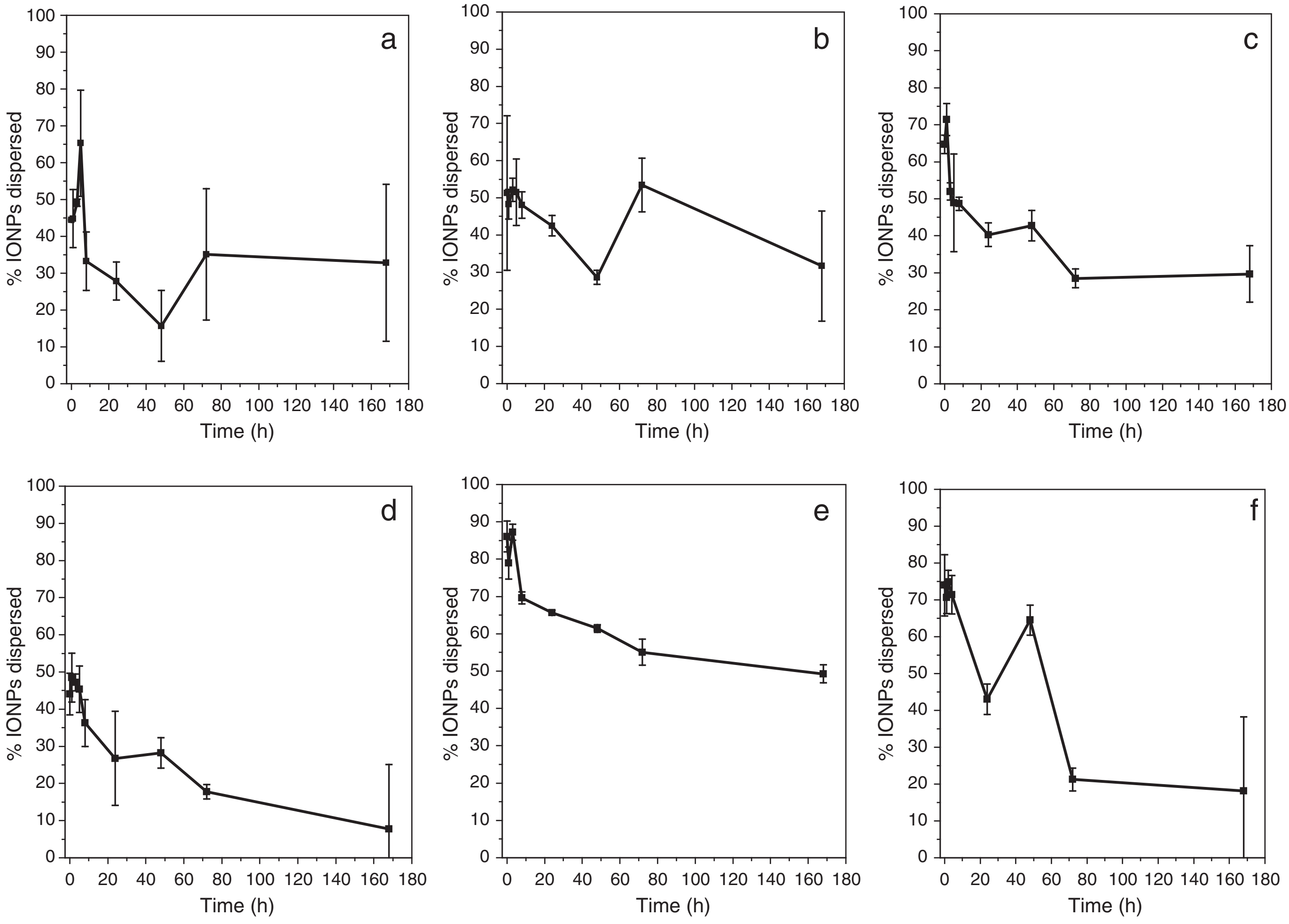

Fig. 2. The percentage of IONPs dispersed over a course of 168 h for a 10 mg/L IONP dispersion at two power levels of sonication and at sonication times of 5, 20 and 60 min. Graphs a, b and c represent dispersion for 5, 20 and 60 min of probe ultrasonication at power level 3. Graphs d, e and f represent dispersion for 5, 20 and 60 min of probe ultrasonication, respectively at power level 6.

to prepare a stable dispersion. There was difficulty dispersing IONPs by vortex as most of the nanoparticles remained aggregated at the bottom of the sample containers and any dispersed particles quickly precipitated. At t_0 (measured immediately following vortex) the average particle diameters ranged from 698 to 2400 nm with smaller sizes observed with increasing time as the larger aggregates sediment leaving the smaller ones remaining in suspension (Fig. 1a). These measured hydrodynamic diameters are significantly larger than the 20–50 nm range reported by the manufacturer. The dilute dispersions (10, 30 and 50 mg/L) had the largest particle size at t_0 while the higher concentrations (75, 100 and 200 mg/L) had smaller sizes. At t_0, we were able to measure the larger particle sizes due to slower aggregation in the lower concentrated dispersions. However, with the highly concentrated dispersions, aggregation and sedimentation occurs at such a fast rate that only the smaller particles remaining in suspension could be measured. The smaller size particles usually remain dispersed due to differential sedimentation because of the polydispersity of the dispersion (Baalousha et al., 2008; Baalousha, 2009). There was always evidence of sedimentation by a deposit of nanoparticles at the bottom of sample containers. Therefore, vortex lacks the capability of breaking up IONP powder and does not sufficiently disperse IONPs. In addition, dispersion by bath sonication was also investigated but rapid sedimentation immediately following sonication (data not shown) limited its capability to disperse IONPs.

Probe ultrasonication was employed as a dispersion tool and IONPs were more uniformly dispersed with smaller hydrodynamic diameter. Fig. 1b shows the change in hydrodynamic diameter with time for different concentrations of IONPs dispersed using ultrasonic probe for 20 min at power level 6. Other power levels and sonication time (5 and 60 min of sonication at both power levels 3 and 6) had similar results (data not shown). Regardless of IONP concentration, probe power level (3 or 6) and time of sonication (5, 20 or 60 min), the particle diameter ranged between 124 and 128 nm at t_0 with minimal changes in size over a period of 168 h. This range of particle size (124–128 nm) was 2–5 times larger than the manufacturers reported primary particle diameter (20–50 nm) and it was slightly greater than the size defined as nanoparticles (<100 nm). For the purpose of easy discussion, we name these particles as nanoparticles in this paper. The ultrasonic probe was a more powerful tool to disperse IONPs when compared to vortex and bath sonication. The difference in dispersion is attributed to the fact that the ultrasonic probe is directly inserted in the sample and it has greater power than the other dispersion methods (Santos and Capelo, 2007). The acoustic waves imparted by ultrasonication is effective in dispersing IONPs due to the transient cavitation and acoustic streaming that can possibly redefine the shape and structure of nanoparticles and change the surface morphology (Suslick and Price, 1999). Specifically, acoustic cavitation gave rise to cavitation cycles that involves the nucleation and collapsing of micro-bubbles creating micro “hot spots” where nanoparticles experience extreme conditions such as high temperatures and pressures. These conditions result in the breakage of aggregated nanoparticles and a more uniform dispersion in liquids (Suslick and Price, 1999; Mandzy et al., 2005).

Although probe ultrasonication broke up the nanoparticles extensively, it could not break down IONPs to the primary particle diameter due to the possible aggregation of the particles during long storage periods (Zhang et al., 2008) or during synthesis (Mandzy et al., 2005) or there could be preexisting aggregates that could not be dispersed by sonication

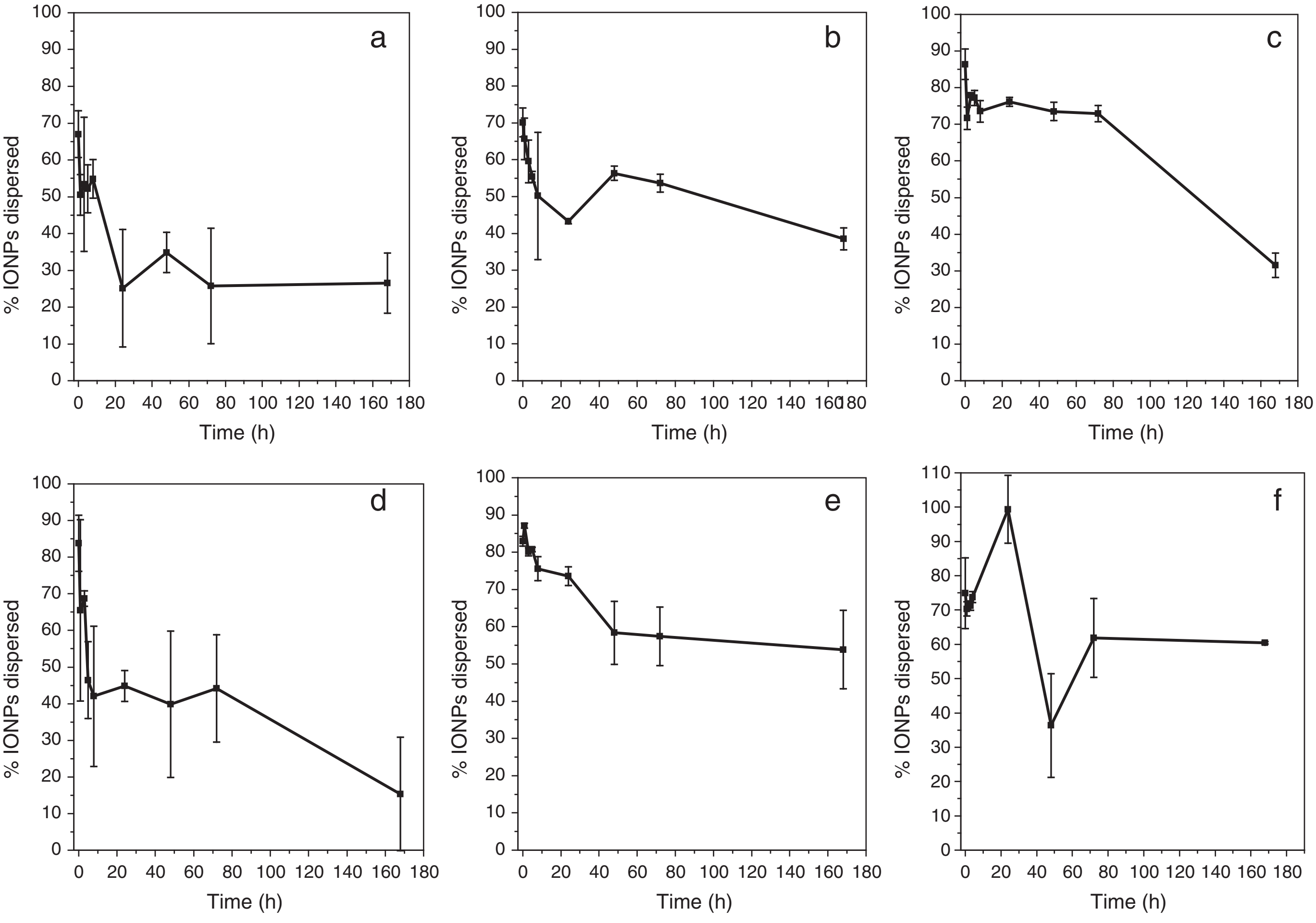

Fig. 3. The percentage of IONPs dispersed over a course of 168 h for a 100 mg/L IONPs dispersed by ultrasonic probe. Graphs a, b and c represent dispersion for 5, 20 and 60 min respectively, at power level 3. Graphs d, e and f represent dispersion for 5, 20 and 60 min, respectively at power level 6.

(Saleh et al., 2005). However the 124–128 nm particle size range obtained in this study was sufficient to evaluate probe ultrasonication as an effective dispersion tool in breaking up nanoparticles and to investigate how the stability of IONPs changes in aquatic environment after being dispersed. Overall, with probe sonication as a dispersion tool, particles with hydrodynamic diameters between 117 and 147 nm remained in suspension over a 168 h time period. Knowing that IONPs were still suspended, it was desirable to quantify the amount of IONPs that remain suspended in order to determine the stability of the IONPs dispersions.

3.2. Stability of IONPs

Nanoparticle stability can be defined as an even distribution of particles throughout the whole volume and the ability of the particles to stay separated from each other with time (Veronovski et al., 2010). However, it is also important that the particle size remains consistent for nanoparticle stability as aggregation to larger particles affects their mobility and reactivity. Although DLS has the ability to measure the hydrodynamic diameter of the particles that were currently suspended, it cannot quantify the amount of IONPs in the dispersion. Therefore, total iron analysis over a period of 168 h was implemented as a means to assess the sedimentation of IONPs as well as to assist in the determination of the appropriate power level and sonication time to disperse IONPs into a stable suspension.

Stability experiments were performed on two concentrations of IONPs: 10 and 100 mg/L. Fig. 2 shows the percentage of IONPs dispersed over a course of 168 h for a 10 mg/L IONPs dispersion at two power levels of sonication and at sonication times of 5, 20 and 60 min. The breakage of IONPs and the amount dispersed was strongly influenced by the energy input of the ultrasonic probe which is controlled by the time, power and dispersion volume (Mandzy et al., 2005). In this experiment, the volume was constant for all samples so the time and power predominantly controlled the amount of IONPs dispersed. The greater the sonication power and the longer the sonication time, the greater the energy input and thus more efficient dispersion. Figs. 2a, 2b and 2c illustrate that an increase in time from 5 to 60 min for power level 3 increased the IONPs dispersion from 44 to 65% at t_0. Similar results were observed for power level 6 as IONPs increased from 44 to 73% with increase in sonication time (Fig. 2d, e and f). In addition an increase in power from level 3 (power density of 0.275 W/mL) to level 6 (power density of 0.55 W/mL) increased the amount of IONPs dispersed at t_0 for sonication times of 20 and 60 min. However, equivalent amount (~44%) of IONPs was dispersed for 5 min of sonication regardless of the power level at t_0. The amount of IONPs dispersed increased from 51% to 86% at 20 min sonication and from 65% to 73% at 60 min when power increased from level 3 to level 6. A similar trend was seen for the 100 mg/L IONPs dispersion, in which the IONPs concentration in the suspension increases as sonication power and time increase (Fig. 3). Monitoring the deposition over time (from t_0 to t_{168}) was important as it will provide information on how long these dispersions will remain stable. As time progressed, aggregation occurred for both the 10 and 100 mg/L IONPs dispersions, as evidenced by the decrease in % IONPs dispersed.

A comparison of the different sonication time at varying power levels indicates that sonicating for 20 min at power level 6 is the optimum dispersion condition. Sonicating for 60 min was time consuming and in most cases only slightly (~15%) increased the amount of IONPs dispersed at t_0 when compared to 20 min. Sonicating for 5 min was not sufficient enough to disperse of the IONPs when compared to the other sonication times, and aggregation and sedimentation were faster compared to the other conditions.

It is important to be aware that a stable size distribution of IONPs in solution does not provide information on the concentration and stability of IONPs. Therefore, it is necessary to monitor the concentration of IONPs in the stability studies. Sedimentation of IONPs is inevitable due to their tendency to aggregate resulted from the electrostatic, steric, and van der Waals forces (Jiang et al., 2009). As shown in this study, size measurements of IONPs at different times had consistent hydrodynamic diameters but particles still aggregate and sediment over time resulting in less and less IONPs being present in the suspensions. As often being overlooked, a stable size distribution does not imply that aggregation and sedimentation of particles do not occur. Monitoring both the particle size distribution and IONPs concentration over time can provide a better estimate on the stability of the dispersions.

3.3. Effect of HA and ionic strength on the stability of IONPs

3.3.1. Effect of HA on IONPs stability

Humic acid is capable of adsorbing on iron oxides and thus can affect the surface charge, reactivity, and stability of the IONPs, which

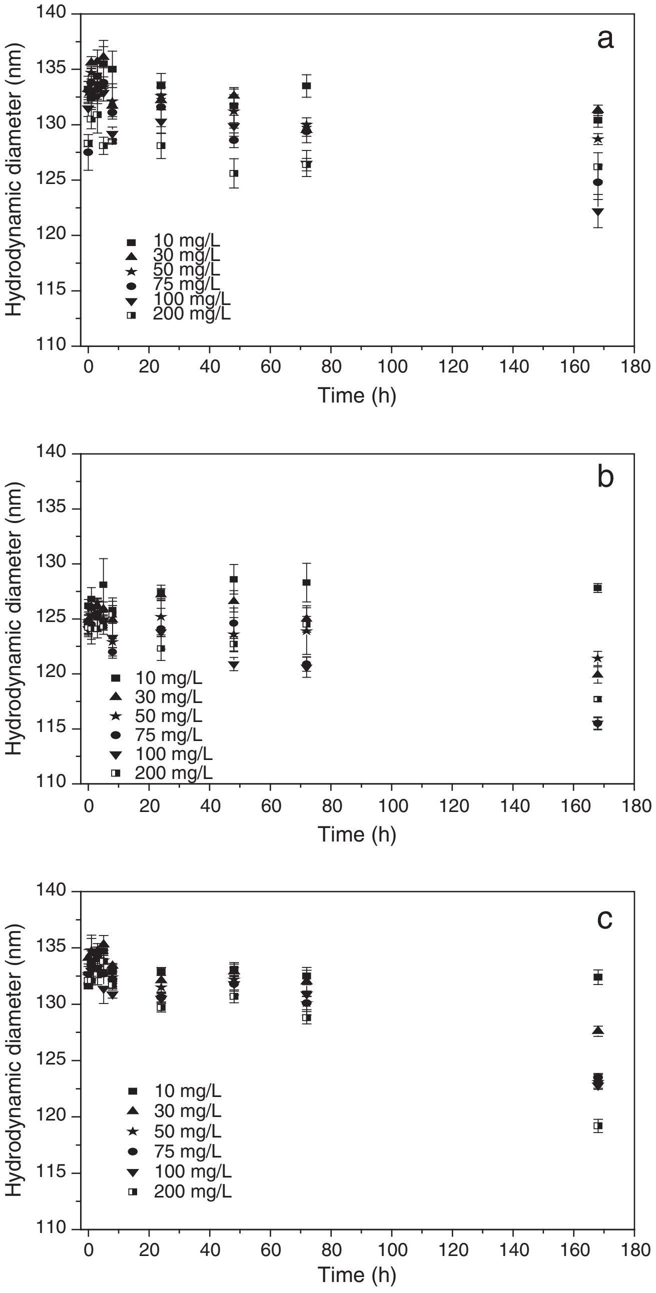

Fig. 4. The time dependent hydrodynamic diameter of 10, 30, 50, 75, 100 and 200 mg/L IONPs dispersed by ultrasonic probe in the presence of different environmental factors a) 100 mg/L HA; b) 0.1 mM NaCl; c) 100 mg/L HA and 0.1 mM NaCl. All samples were dispersed using ultrasonic probe for 20 min at power level 6.

subsequently could influence the interaction of IONPs with metal contaminants (Mylon et al., 2004; Liu and Cai, 2010; Liu et al., 2011). Our study indicates that there was no significant change in the size of IONPs when HA was present. The hydrodynamic diameter ranged from 128 to 133 nm at t_0 with the sizes slightly decreasing over the next 168 h for all concentrations of IONPs (Fig. 4a.). It was reported that the hydrodynamic radius between hematite colloids and natural organic matter (NOM) coated hematite was indistinguishable when using DLS measurements. It was reported that HA increased the layer thickness of small hematite colloids by only <2 nm (Au et al., 1999; Mylon et al., 2004).

Monitoring the IONP concentration with time indicated that 70% or more IONPs were dispersed for all IONP suspensions at t_0 regardless of the nanoparticle concentration (dash lines in Fig. 5). There was minimal sedimentation of IONPs from t_0 to t_{168} with approximately 10–15% of IONPs sediment. The minimal sedimentation could be a result of the decrease in aggregation of the IONPs in the presence of HA resulting from the possibly coating of HA on the surface of the nanoparticles. It has been reported that HA can coat the surface of the nanoparticle thereby preventing aggregation through either electrostatic or steric interactions (Ghosh et al., 2010). Hematite nanoparticles have a point of zero charge (PZC) ranging from pH 5.5 to 9.5 depending on the method of synthesis and experimental conditions (Schwertmann and Cornell, 2000; He et al., 2008; Cerovic et al., 2009; Shipley et al., 2010). At this pH of 5.5 to 9.5, the repulsive force between IONPs decreases due to the lack of charge on the IONPs surface resulting in aggregation of the particles. Therefore the IONPs used in this study should experience a high degree of instability since all the samples in this study have measured pH ranging from pH 6.2–7.6, which is within the PZC range of hematite nanoparticles (pH 5.5–9.5). Zeta potential measurements showed that the uncoated IONPs had a slight positive charge with zeta potential $+29.8 \pm 0.9$ mV, while the HA coated IONPs were more negatively charged with a zeta potential of -48.0 ± 0.6 mV. HA has an abundance of carboxylic ($-$COOH, -COO$^-$) and phenolic ($-$OH) functional groups that exist as negatively charged and it is believed that HA coating the surface can suppress any positive charge of the nanoparticle while enhancing the negative charge (Illes and Tombacz, 2006; Christian et al., 2008; Hu et al., 2010). Therefore, the minimal sedimentation of IONPs in the presence of HA (Fig. 5) compared to that without HA (Figs. 2 and 3) could be explained by HA coating the IONPs surface leading to a change in the surface charge of the IONPs

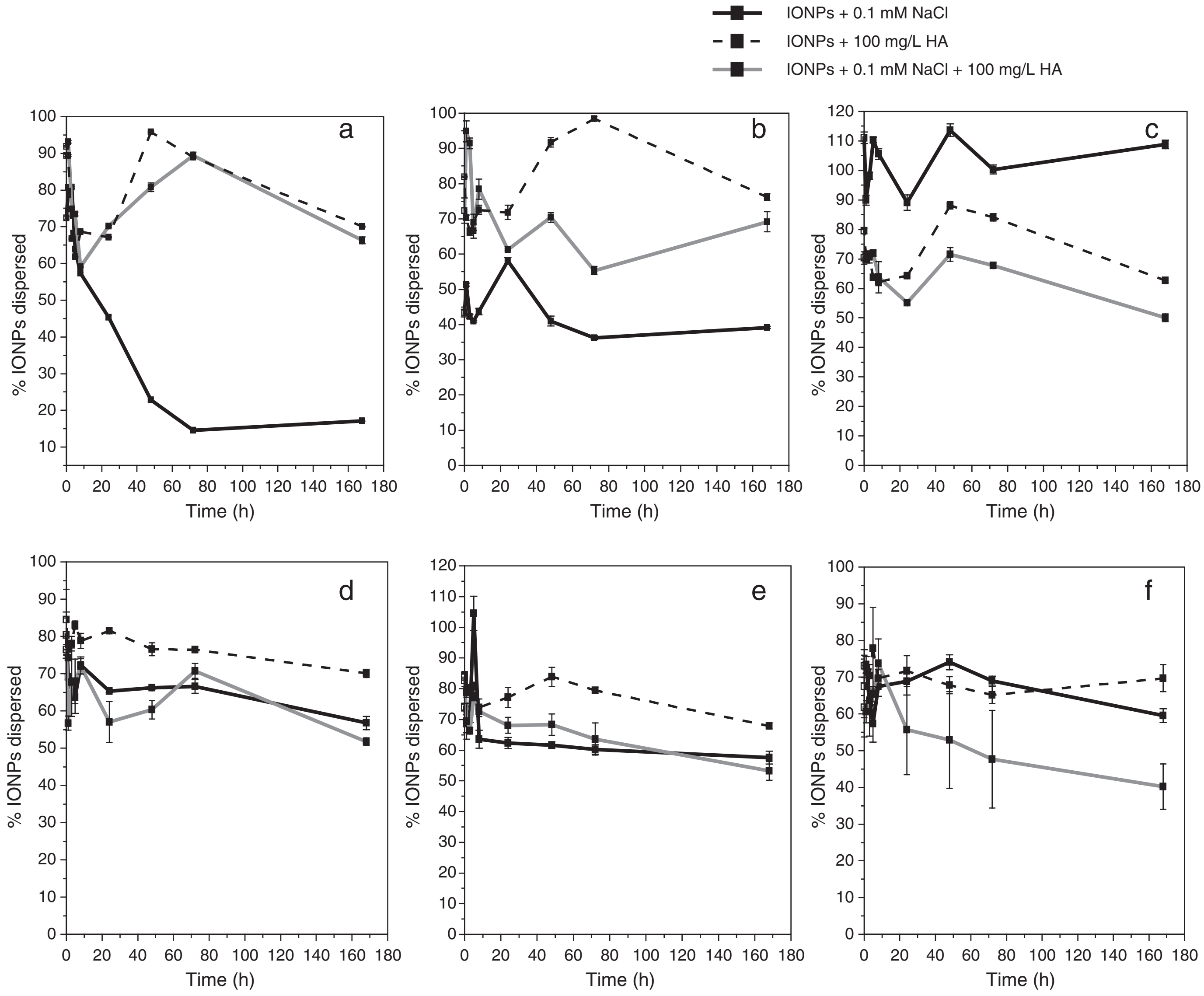

Fig. 5. The percentage of IONPs dispersed over a course of 168 h while investigating the effect of 0.1 mM NaCl and 100 mg/L HA (alone or in combination) on the dispersion of IONPs. Graphs a, b, c, d, e and f represent the percentage of IONPs dispersed in 10, 30, 50, 75, 100 and 200 mg/L IONPs suspension respectively. All samples were dispersed using ultrasonic probe for 20 min at power level 6.

from a slightly positive charge to a stronger negative charge. The stronger negative charge with HA present possibly has a greater repulsive force compared to the slightly positive charge of IONPs without HA, thus enhancing stability through electrostatic interactions (Ghosh et al., 2010).

3.3.2. Effect of ionic strength on IONPs stability

The DLVO theory can be used to explain the stability of IONP dispersions. The van der Waals attractive forces and electrical double layer repulsive force between particles play a significant role in controlling the aggregation of particles. The ionic strength has a strong influence on the thickness of the electrical double layer. An increase in ionic strength would lead to a decrease in the electric double layer thickness resulting from the compression of the electric double-layer causing aggregation of particles (Zhang et al., 2008; Jiang et al., 2009). To examine the effect of ionic strengths on IONPs aggregation, several concentrations of NaCl (0.1, 10 and 100 mM) were tested.

At low ionic strength (0.1 mM), the hydrodynamic diameter ranged from 115 to 130 nm (Fig. 4b) over the course of 168 h. These results were not significantly different from the size of IONPs alone (Fig. 1b), indicating that at low ionic strength, the electrostatic repulsive force is dominant over the attractive force therefore the particle size was not altered. In regards to the quantity of IONPs suspended over time, Fig. 5 (dark solid lines) shows that approximately 50% or more IONPs were dispersed for the 10, 30, 50, 75, 100 and 200 mg/L dispersions. Majority of the IONPs had remained dispersed with only 10–15% deposition of IONPs from t_0 to t_{168} for all IONPs concentration except for the 10 mg/L dispersion (Fig. 5). The 10 mg/L dispersion had the greatest sedimentation over time and this could possibly be a result of a concentration effect (see below). Similar to the addition of 0.1 mM NaCl to the nanoparticle suspension, the addition of 10 mM NaCl resulted in aggregation and sedimentation that depended upon the nanoparticle concentrations (data not shown). An increase in ionic strength to 10 mM NaCl resulted in rapid aggregation and sedimentation for the 10, 30, 50 and 75 mg/L IONPs dispersion within 8 h as evidenced by a deposit of nanoparticles at the bottom of sample containers as well as unsuccessful DLS measurements due to the intensity of the scattered light not satisfactory for quantitative determination of particle size. However, the 100 and 200 mg/L suspensions were not significantly affected and were stable for DLS measurements (Fig. 6). These results could possibly be accounted for by the compression of the electric double layer being more feasible in low IONP concentration at the same ionic strength, resulting in fast aggregation of the nanoparticles.

A further increase in ionic strength (100 mM) caused rapid aggregation and sedimentation of all the IONPs dispersions within 4 h. Similarly to 10 mM ionic strength, deposits of nanoparticles accumulated at the bottom of sample containers and DLS measurements were unsuccessful due to the polydispersity of the suspensions. At this ionic strength, van der Waals attractive forces dominate over the repulsive forces causing significant aggregation. Furthermore, metal oxides have large Hamaker constants (Petosa et al., 2010) and electrostatic stabilization is usually achieved at low ionic strength which is agreeable with our findings.

3.3.3. Stability of IONPs in the presence of both HA and low ionic strength

The aggregation behavior of IONPs was investigated in the coexistence of low ionic strength (0.1 mM NaCl) and HA. Fig. 4c shows that the hydrodynamic diameters ranged from 132 to 135 nm at t_0 with sizes decreasing slightly over the course of 168 h. These sizes are similar to the hydrodynamic diameter of IONPs in the presence of HA alone (128–133 nm, Fig. 4a) and in the presence of low ionic strength alone (115–130 nm, Fig. 4b). The amount of nanoparticles dispersed was 65% or more at t_0 with minimal sedimentation for all IONPs over 168 h (Fig. 5, light solid lines). The large sedimentation of IONPs that was seen for the 10 mg/L dispersion in the presence of 0.1 mM NaCl alone, was not observed when both HA and NaCl were present. The instability caused by the ionic strength could have been overcome by the stabilization effect of HA. Overall, the minimal sedimentation could be a result of HA coating the surface of the nanoparticles causing both steric and electrostatic stabilization as well as the ionic strength being low enough to allow for electrostatic repulsive force to be dominant therefore enhancing the stability of IONPs. Therefore, IONP dispersions can be prepared under different environmental factors with these dispersions being stable for a prolonged period of time.

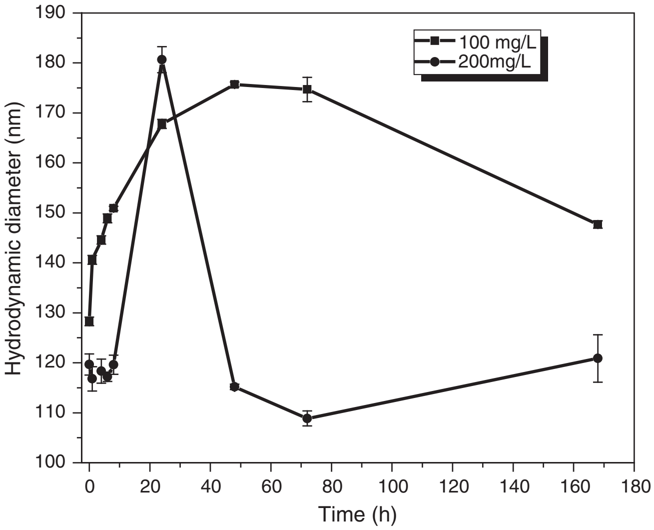

Fig. 6. The time dependent hydrodynamic diameter of 100 and 200 mg/L IONP dispersions in the presence of 10 mM NaCl. Samples were dispersed using ultrasonic probe for 20 min at power level 6.

4. Conclusions

In this study, we determined that probe ultrasonication is an appropriate tool to disperse IONPs. Although probe ultrasonication did not break the IONPs down into the primary particle size, this method had proven to be more effective in dispersing IONPs compared to dispersion via vortex or bath sonication. It is important to be aware that a stable *size* distribution of IONPs in solution does not necessarily correlate with the *concentration* of IONPs therefore it is necessary to monitor the concentration of IONPs in stability studies. An increase in ultrasonication time and power increased the amount of IONPs dispersed. Although sedimentation occurred to some extent, a considerable amount of IONPs remained in suspension in the presence and absence of 100 mg/L HA and 0.1 mM NaCl. Results showed that high ionic strengths increased colloidal instability by compressing the electrical double layer thickness causing rapid aggregation and sedimentation. On the other hand, the electrostatic repulsive force dominated at low ionic strengths resulting in reduced destabilization of the dispersions. The addition of modifiers to enhance stability of IONPs may not be necessary as the presence of HA, which is naturally found in the environment, could enhance the colloidal stability of IONPs through possible steric and electrostatic repulsion. These results are important as stable IONPs dispersions can be prepared without the use of synthetic modifiers. This research provides us with a useful tool for development of a laboratory scale methodology to study and understand the adsorption mechanisms of toxic environmental contaminants with unmodified IONPs.

Acknowledgments

This work was supported by NIH-NIEHS ARCH (S11ES11181). Dionne Dickson would like to acknowledge the Florida International

University for financial support. This is contribution no. 539 of the Southeast Environmental Research Center at FIU.

References

Au K-K, Penisson AC, Yang S, O'Melia CR. Natural organic matter at oxide/water interfaces: complexation and conformation. Geochim Cosmochim Acta 1999;63:2903–17.

Baalousha M. Aggregation and disaggregation of iron oxide nanoparticles: influence of particle concentration, pH and natural organic matter. Sci Total Environ 2009;407:2093–101.

Baalousha M, Manciulea A, Cumberland S, Kendall K, Lead JR. Aggregation and surface properties of iron oxide nanoparticles: influence of pH and natural organic matter. Environ Toxicol Chem 2008;27:1875–82.

Cerovic L, Lefevre G, Jaubertie A, Fedoroff M, Milonjic S. Deposition of hematite particles on polypropylene walls in dynamic conditions. J Colloid Interface Sci 2009;330:284–91.

Christian P, Von der Kammer F, Baalousha M, Hofmann T. Nanoparticles: structure, properties, preparation and behavior in environmental media. Ecotoxicology 2008;17:326–43.

Deryagin B, Landau L. Theory of the stability of strongly charged lyophobic sols and of the adhesion of strongly charged particles in solutions of electrolytes. Acta Physicochim 1941;14:633–62.

Ghosh S, Mashayekhi H, Bhowmik P, Xing B. Colloidal stability of Al_2O_3 nanoparticles as affected by coating of structurally different humic acids. Langmuir 2010;26:873–9.

He F, Zhao D. Manipulating the size and dispersibility of zerovalent iron nanoparticles by use of carboxymethyl cellulose stabilizers. Environ Sci Technol 2007;41:6216–21.

He YT, Wan J, Tokunaga T. Kinetic stability of hematite nanoparticles: the effect of particle sizes. J Nanopart Res 2008;10:321–32.

Hu J-D, Zevi Y, Kou X-M, Xiao J, Wang X-J, Jin Y. Effect of dissolved organic matter on the stability of magnetite nanoparticles under different pH and ionic strength conditions. Sci Total Environ 2010;408:3477–89.

Illes E, Tombacz E. The effect of humic acid adsorption on pH-dependent surface charging and aggregation of magnetite nanoparticles. J Colloid Interface Sci 2006;295:115–23.

Jiang J, Oberdorster G, Biswas P. Characterization of size, surface charge, and agglomeration state of nanoparticle dispersions for toxicological studies. J Nanopart Res 2009;11:77–89.

Kanel SR, Nepal D, Manning B, Choi H. Transport of surface-modified iron nanoparticle in porous media and application to arsenic(III) remediation. J Nanopart Res 2007;9:725–35.

Kim H-J, Phenrat T, Tilton RD, Lowry GV. Fe^0 nanoparticles remain mobile in porous media after aging due to slow desorption of polymeric surface modifiers. Environ Sci Technol 2009;43:3824–30.

Liu G, Cai Y. Complexation of arsenite with dissolved organic matter: conditional distribution coefficients and apparent stability constants. Chemosphere 2010;81:890–6.

Liu J-f, Zhao Z-s, Jiang G-b. Coating Fe_3O_4 magnetic nanoparticles with humic acid for high efficient removal of heavy metals in water. Environ Sci Technol 2008;42:6949–54.

Liu G, Fernandez A, Cai Y. Complexation of arsenite with humic acid in the presence of ferric iron. Environ Sci Technol 2011;45:3210–6.

Mandzy N, Grulke E, Druffel T. Breakage of TiO_2 agglomerates in electrostatically stabilized aqueous dispersions. Powder Technol 2005;160:121–6.

Mylon SE, Chen KL, Elimelech M. Influence of natural organic matter and ionic composition on the kinetics and structure of hematite colloid aggregation: implications to iron depletion in estuaries. Langmuir 2004;20:9000–6.

Petosa AR, Jaisi DP, Quevedo IR, Elimelech M, Tufenkji N. Aggregation and deposition of engineered nanomaterials in aquatic environments: role of physicochemical interactions. Environ Sci Technol 2010;44:6532–49.

Phenrat T, Saleh N, Sirk K, Tilton RD, Lowry GV. Aggregation and sedimentation of aqueous nanoscale zerovalent iron dispersions. Environ Sci Technol 2007;41:284–90.

Phenrat T, Liu Y, Tilton RD, Lowry GV. Adsorbed polyelectrolyte coatings decrease Fe nanoparticle reactivity with TCE in water: conceptual model and mechanisms. Environ Sci Technol 2009;43:1507–14.

Rangsivek R, Jekel MR. Natural organic matter (NOM) in roof runoff and its impact on the Fe^0 treatment system of dissolved metals. Chemosphere 2008;71:18–29.

Saleh N, Phenrat T, Sirk K, Dufour B, Ok J, Sarbu T, et al. Adsorbed triblock copolymers deliver reactive iron nanoparticles to the oil/water interface. Nano Lett 2005;5:2489–94.

Santos HM, Capelo JL. Trends in ultrasonic-based equipment for analytical sample treatment. Talanta 2007;73:795–802.

Schrick B, Hydutsky BW, Blough JL, Mallouk TE. Delivery vehicles for zerovalent metal nanoparticles in soil and groundwater. Chem Mater 2004;16:2187–93.

Schwertmann U, Cornell RM. Iron oxides in the laboratory: preparation and characterization. Weinheim: Wiley; 2000.

Shipley H, Engates K, Guettner A. Study of iron oxide nanoparticles in soil for remediation of arsenic. J Nanopart Res 2010;13:2387–97.

Sun Y-P, Li X-q, Cao J, Zhang W-x, Wang HP. Characterization of zero-valent iron nanoparticles. Adv Colloid Interface Sci 2006;120:47–56.

Sun Y-P, Li X-Q, Zhang W-X, Wang HP. A method for the preparation of stable dispersion of zero-valent iron nanoparticles. Colloids Surf, A 2007;308:60–6.

Suslick KS, Price GJ. Applications of ultrasound to materials chemistry. Annu Rev Mater Sci 1999;29:295–326.

Theron J, Walker JA, Cloete TE. Nanotechnology and water treatment: applications and emerging opportunities. Crit Rev Microbiol 2008;34:43–69.

Tiraferri A, Chen KL, Sethi R, Elimelech M. Reduced aggregation and sedimentation of zero-valent iron nanoparticles in the presence of guar gum. J Colloid Interface Sci 2008;324:71–9.

Veronovski N, Andreozzi P, La Mesa C, Sfiligoj-Smole M. Stable TiO_2 dispersions for nanocoating preparation. Surf CoatTechnol 2010;204:1445–51.

Verwey EJW. Theory of the stability of lyophobic colloids. J PhysColloid Chem 1947;51:631–6.

Verwey EJW, Overbeek JTG. Theory of the stability of lyophobic colloids. Elsevier: Amsterdam; 1948.

Wang C-B, Zhang W-x. Synthesizing nanoscale iron particles for rapid and complete dechlorination of TCE and PCBs. Environ Sci Technol 1997;31:2154–6.

Yang GCC, Tu H-C, Hung C-H. Stability of nanoiron slurries and their transport in the subsurface environment. Sep Purif Technol 2007;58:166–72.

Zhang Y, Chen Y, Westerhoff P, Hristovski K, Crittenden JC. Stability of commercial metal oxide nanoparticles in water. Water Res 2008;42:2204–12.